Ferritic Insertion for Reduction of Toroidal Magnetic Field Ripple on JT-60U

K. Shinohara 1), S. Sakurai 1), M. Ishikawa 1), K. Tsuzuki 2), Y. Suzuki 1), K. Masaki 1), O. Naito 1), K. Kurihara 1), T. Suzuki 1), Y. Koide 1), T. Fujita 1), Y. Miura 1), and the JT-60 Team 1)

1) Japan Atomic Energy Agency, Naka, Ibaraki-ken 311-0193, Japan
2) The Institute of Applied Energy, 1-14-2 Nishi-shimbashi, Minato-ku, Tokyo 105-0003, Japan

e-mail contact of main author: shinohara.koji@jaea.go.jp

Abstract. Ferritic steel tiles (FSTs) have been installed in order to improve the energetic ion confinement through reducing a toroidal magnetic field ripple. Aiming at cost-effective installation, orbit following calculations of energetic ions were carried out for a design of FST installation on JT-60U by using the Fully three Dimensional magnetic field Orbit-Following Monte-Carlo (F3D OFMC) code, which had been developed for ferritic insert experiments on JFT-2M and can treat complex magnetic field structure produced by ferritic inserts. The installed FSTs add the non-linear magnetic field on magnetic sensors for a plasma control and an equilibrium calculation. The code for a real-time control has been modified to take into account the magnetic field by FSTs. The plasma operation was successfully resumed after usual conditioning processes and a real-time plasma control was successfully carried out. The heat load measurement indicates the improved confinement of energetic ions. These results are important for practical application of ferritic steel, which is a leading candidate of a structural material on a demo reactor.

1. Introduction

Due to the discreteness of the toroidal magnetic field (TF) coil system, the TF coil system produces TF ripple, which is a ripple-shape non-uniformity of TF strength. The TF ripple induces loss of energetic ions due to the lack of the up-down symmetry of banana orbit (banana diffusion) or due to local mirror trapping (ripple trapped loss). These losses reduce the “effective” efficiency of plasma heating through reducing the number of confined energetic particles. The TF ripple induces not only the moderate degradation, but also the serious damage on the system. The ripple trapped loss of energetic particles can create a large localized heat load on the first wall, which could induce an unacceptable heat load on the first wall. Thus, the TF ripple was one of the important issues in the ITER design to be well analyzed, and has been investigated theoretically and experimentally [1-3].

To avoid the unfavorable effect of TF ripple, it is effective to reduce the amplitude of TF ripple itself. One method is the adjustment of TF coil set-up, such as to increase the number or the width of TF coils, and another one is to use the ferromagnetic material. The former one not only reduces the accessibility of diagnostics, heating/current drive systems and maintenance systems by reducing the area of ports, but also is relatively expensive. The latter one was not tried on any tokamak until its recent installation on the middle-sized JFT-2M tokamak [4, 5]. Because the magnetic field created by ferromagnetic material is complex (an example is shown in FIG. 1 (c)) due to a limitation of its realistic installation, and it was suspected that the field could be the source of the error field, which could affect the MHD stability.

On the JFT-2M, the effectiveness of the ferromagnetic material for the improvement of energetic ion confinement was demonstrated on an actual tokamak for the first time. As a result of the ripple reduction, a temperature increment on the first wall, which indicates the

ripple-induced loss of energetic ions, was also reduced. However, this result was not self-evident because the magnetic structure produced by the ferritic steel was complex. To analyze the energetic ion behavior in the complex magnetic field, a new version of the OFMC code, the Fully Three-Dimensional magnetic field (F3D) OFMC code, had been also developed, in which the three-dimensional complex structure of the toroidal field ripple and the wall shape were included [6].

On the basis of these pioneering works on the JFT-2M, the installation of ferritic steel was proposed on the JT-60U. The main target of this installation on the JT-60U is to utilize large volume plasmas, in which the effect of the TF ripple is large, in order to reach more steady-state, high-beta plasmas, because large volume plasmas benefit from wall-stabilization and from a good coupling with the RF heating/current-drive system.

The design work was carried out aiming at an effective and short-term installation with keeping a similar operational region. In the design work, the enhanced confinement of energetic ions and the absence of unfavorable heat flux on the first wall were assessed by using the F3D OFMC code mentioned above.

On the JFT-2M, the precise control in a real time was not required because the inappropriate operation did not lead to serious machine problems. On the other hand, on the JT-60U, the plasma current, the TF strength, and the net energy are so large that the disruption due to the inappropriate operation could lead to serious machine problems. Thus, a plasma control using a real-time computer calculation is performed, while a plasma control using an analog circuit was applied on the JFT-2M. The real-time calculation of the plasma shape was carried out by using magnetic sensor signals, and the poloidal and toroidal coil currents. After the installation of ferritic steel tiles (FSTs), FSTs produce the additional magnetic field at magnetic sensors. Furthermore, FSTs produce the additional magnetic field at the plasma position. The plasma shape control that takes into account the effect of FSTs is required to calculate the plasma shape with good accuracy. Such plasma control scheme has been implemented on the JT-60U.

Here, we describe the technical implementation for the ferritic steel. The design procedure of the FST installation will be shown in Sec. 2. The assessment of the improvement of the energetic ion confinement and the mechanical requirement will be discussed. The real-time control system and the equilibrium calculation under the environment with FSTs will be described in Sec. 3. In Sec. 4, initial experimental results will be shown from the viewpoint of interest and concern related to the ferritic insertion.

2. Ferritic insertion to improve energetic ion confinement in large volume plasmas

The installation of ferritic steel was proposed to reduce the TF ripple. The reduction of energetic ion loss due to the TF ripple reduction is expected to bring: 1) The improved heating and current drive “effective” efficiency. The ripple reduction improves the confinement of NB ions. The ratio of the absorbed power to the deposited power is expected to increase. 2) The extended pulse length and the improved efficiency of the RF injection. The large heat load on RF antennas is mainly coming from escaping energetic ions [3,8]. The reduction of the heat load due to the enhanced confinement of energetic ions will allow the improved coupling between antennas and plasma is expected. 3) The availability of wall stabilization without losing heating power due to the enhanced confinement of energetic ions in large volume plasmas. 4) The possibility of the enhanced availability of the rotation control to

improve the MHD stability and transport.

It is expected that the above-mentioned benefits will be brought mainly in large volume plasmas, where the ripple amplitude was relatively large with TF coils alone. Thus, our assessment of the energetic ion confinement has been carried out intensively for a large volume plasma configuration, which is shown in FIG. 1(a). The assessment of the energetic ion confinement was carried out by using the F3D OFMC code [6, 9]. Major guidelines of our installation were 1) to keep an operation domain of 3 MA / 4 T with a resistance to a disruption, 2) to avoid the interference with the existing equipments, and 3) a cost-effective short-term installation. Because of the second guideline, the ferritic steel needed to be installed inside a vacuum vessel. We did not hesitate to install the ferritic steel inside the vacuum vessel due to the experience on JFT-2M. We carried out quantitative assessments of energetic ion confinement for a several trial designs from qualitative considerations, considering these requirements.

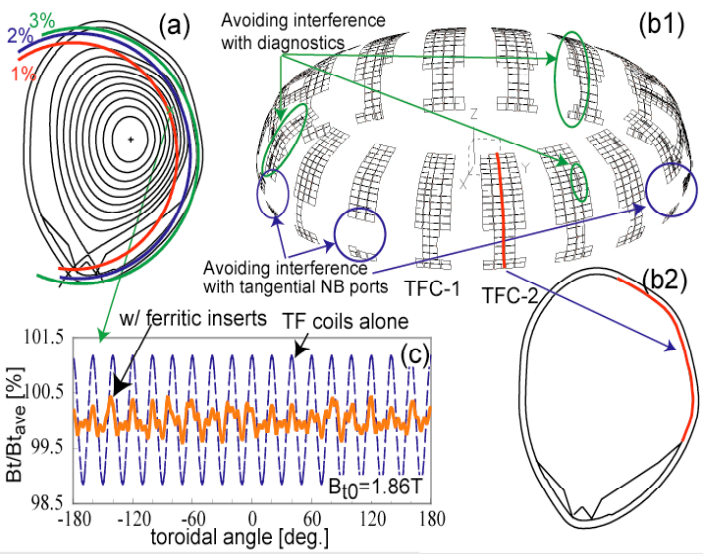

FIG. 1. (a) Plasma configuration with ripple rate contour for TF coils alone, Bt_0=1.9T, Ip=1.1MA, q_{95}=3.4, plasma volume =79m^3, line averaged electron density ~1.5 x$10^{19}m^{-3}$, central electron temperature ~ 6 keV. (b1) A bird's eye view of the installed FSTs in the final design. Periodic installation was essentially difficult to be compatible with other equipments, (b2) A poloidal cross section of the installed FSTs under one of TFC for the final design, (c) Toroidal variation of TF strength at R= 4.2 m and Z= 0.6 m for Bt_0= 1.86 T shown by percentage.

The final design is shown in FIG 1(b1), (b2). The FSTs with the ingredient of 8%Cr-2%W-0.2%V[10], whose saturation magnetization is about 1.7 T at 573 K, were installed in place of graphite armors as the first wall by about 10 % surface area. This steel has a similar saturation magnetization to F82H ferritic steel (8Cr-2W-0.2V-0.04Ta), which is reduced-activation ferritic steel developed by JAERI (present abbreviated name is JAEA) and NKK. The FSTs are placed at the upper part of a vacuum vessel in the low field side and under TF coils. In FIG. 1(c), the resultant variation of the TF strength at R= 4.2 m, Z= 0.6 m is compared with

TABLE 1: COMPARISON OF SIMULATION RESULTS FOR ABSORBED POWER AND LOSS POWER BETWEEN WITHOUT AND WITH FSTS. POWER FRACTION IS THE RATIO TO THE DEPOSITED POWER IN PLASMA, NOT TO THE INJECTION POWER

	Absorbed power for full injection [%]	Loss power for full injection [%]	Absorbed power for perp. PNB [%]	Absorbed power for co-tan. PNB [%]	Absorbed power for ctr-tan. PNB [%]	Absorbed power for co-tan. NNB [%]
w/o FSTs	54	46	40	73	59	75
w/ FSTs	68	32	58	84	67	84

that of TF coils alone. The reduction of variation amplitude is by about 1/4. The absorbed power calculated by F3D OFMC for this design is compared with that for the case without the FSTs in Table 1. The improvement of the absorbed power to the plasma was evaluated to be a factor of about 1.3 in the case of full injection of neutral beams (NBs), where 7 beams are perpendicular positive-ion-based NBs (PNBs), 2 beams are co-tangential PNBs, 2 beams are counter-tangential PNBs, and 2 beams are co-tangential negative-ion-based NBs (NNBs) (co- and counter- mean the same and opposite direction to a plasma current, respectively.) In this assessment, each PNB has the injection energy of 85 keV and the injection power of 2.25 MW and each NNB has the injection energy of 350 keV and the injection power of 2 MW. The effect of the ripple induced loss is large for perpendicular beams because the orbits of the most beam ions are a banana shape. Thus, the improvement of energetic ions was larger for the perpendicular-injected PNBs. The improvement was a factor of about 1.5. Interestingly, the improvement was observed somewhat even for co-tangential NBs.

The installation of FSTs on a part of the baffle board of a divertor and on the ceiling of the vacuum vessel was assessed in trial calculations, expecting the reduction of the ripple induced loss. The improvement of the energetic ion confinement due to the installation on these areas was small, while the cost for the installation increased much. Through these trials, we considered that the final design was the cost-effective one.

The magnetic field produced by FSTs is saturated above the external vacuum magnetic field of about 0.6 T with the saturation magnetization of about 1.7 T at 573 K. The magnetic field produced by FSTs is almost constant in the typical operational toroidal magnetic field, namely > 1T, on the JT-60U. This means that the FSTs might “over-cancel” the TF ripple in the lower magnetic field and work less effectively in the higher magnetic field. The energetic ion confinement in the different strength of the toroidal magnetic field at the machine center (R=3.32 m, Z=0 m), Bt_0, of 1.2T, 1.6T, 2.6T and 3.3T was calculated. The plasma current and poloidal coil current varied depending on the value of the toroidal field. Namely, the profile of the safety factor, q, is the same. FIG. 2 shows the variation of the absorbed power fraction for cases with and without the FSTs and the ratio of the absorbed power with the FSTs to that without the FSTs. The ferritic insertion is less effective for the cases of 2.6T and 3.3T, compared with the case of < 2T. Even so, the absorbed power is enhanced by about a factor of 1.2 for both the cases of 2.6T and 3.3T. The enhancement of the absorbed power is still observed for 1.2T in this configuration, though the over-cancel of the TF ripple is observed. It is expected that the ferritic insertion is effective in the wide range of the operational TF strength.

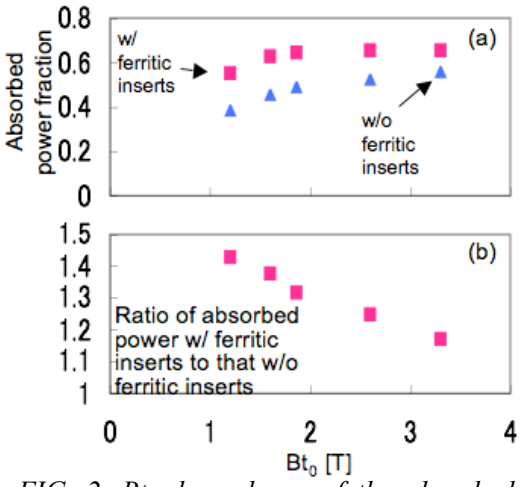

FIG. 2. Bt_0 dependence of the absorbed power fraction for cases with and without FSTs, (a), and the ratio of the absorbed power with FSTs to that without FSTs, (b).

To install the FSTs safely, the mechanical assessment was also carried out. The first concern was the increase of electromagnetic force due to eddy current because the resistivity was much reduced from 9 μΩm (carbon armors) to 0.49 μΩm (8Cr-2W-0.2V). Thus, slits were introduced to avoid the rupture of the stud by the electromagnetic force. And the weight of a piece of FST is roughly 4 kg and triple of the graphite armors. Maximum loads of each plate are evaluated at maximum acceleration load of the vacuum vessel [11] and static magnetic force and maximum eddy current of each plate derived with a simple model.

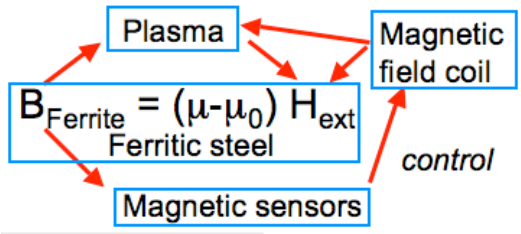

FIG. 3. Schematic diagram about the effect of ferritic steel on plasma.

Maximum loads reach several times of those for graphite armors. The existing stud nuts for fixing armors are reinforced, and high tension bolts are used in order to avoid large modification of existing equipments installed under armors. Inlay structure between a plate, a base and a reinforced stud nut is also applied to reduce large load to a bolt in the poloidal direction [12].

As a result of the assessment for the cost effective installation, the modification was minimized. The replacement of graphite armors with FSTs started in January 2005 and had been finished in August 2005.

3. Development of plasma control scheme and code for equilibrium calculation

On a large tokamak, a precise plasma control is especially important to avoid an accidental damage because of large plasma current and a large TF strength. A plasma shape also determines energy confinement performance, stability, and safe operation. The plasma control and the calculation of the plasma equilibrium are based on the magnetic sensor measurement. So far, the sensors detected the magnetic field from a plasma and poloidal coils. Under the environment with FSTs, the sensor additionally picks up the magnetic field produced by the FSTs. The magnetic field by the FSTs is a production of the interaction between the FSTs and the plasma, and between the FSTs and the poloidal coils. Thus, the magnetic field by the FSTs affects the control and the equilibrium calculation non-linearly (FIG. 3). The real-time control could be difficult when the non-linearity were strong. The strength of the non-linearity had been marginal on the preliminary rough estimation.

In JT-60U, the code for the real-time plasma position and shape control is based on the Cauchy Condition Surface (CCS) method[13]. We revised the code using the following model, considering the available computing resources in the real-time control. In the model, the contribution from the FSTs is evaluated by using the functions as shown in eq. 1, which were made through the numerical simulation and the fitting of the numerical results.

$$\psi_{fe}{}^{j}(t) \approx \sum_i \mathrm{f}_i{}^{j}\left(\vec{B}_{ext}\left(\vec{X}_i, t-\Delta t\right)\right), \quad \vec{B}_{fe}{}^{j}(t) \approx \sum_i \mathrm{g}_i{}^{j}\left(\vec{B}_{ext}\left(\vec{X}_i, t-\Delta t\right)\right) \qquad \text{(eq. 1)},$$

Here, Ψ_{fe} is a magnetic flux by FSTs, B_{fe} is a magnetic field by FSTs, i is the group number (FSTs are divided into four groups in poloidal direction, considering computing resources). j is the index of mesh point at plasma region and each magnetic sensor. Δt is a calculation interval of CCS control system and 1ms in JT-60U. X_i shows representative position of group i and B_{ext} is the external magnetic field at each group due to plasma current and poloidal field coils, which is derived from CCS calculation results just before the time slice, namely Δt before the time slice.

In the numerical simulation, magnetic flux at plasma region by FSTs and magnetic field at most of B_θ probes were evaluated with the magnetic charge approximation code FEMAG [14] because the plasma region is far from the FSTs. On the other hand, magnetic field at some B_θ probes beneath FSTs is very sensitive to the neighboring plate shape and a distance between a probe and plates. Therefore, magnetic field at the B_θ probes is an addition of the following two components. The first component is the magnetic field by neighboring plates. This component is calculated using a precise plate shape and distance with the finite elements method electro-magnetic analysis code EMSolution [15]. And the second component is the magnetic field by plates excluding the neighboring plates. This component is calculated by using the FEMAG code.

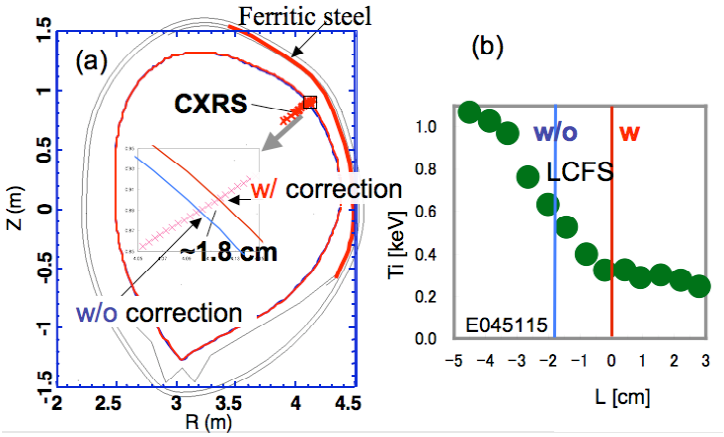

FIG. 4. (a) calculated LCFS with and without correction for effect of FSTs. (b) comparison between Ti profile and LCFS position in H-mode plasma.

In order to reduce calculation time for a real time plasma control, functions f_i^j and g_i^j in eq. 1 are expressed by polynomial approximate expressions by the least square fitting of simulation results from the FEMAG and EMSolution calculation.

Using this modified code, we evaluated the effect of FSTs. In the case of JT-60U, the effect of the magnetic field by FSTs is very small, less than 0.5 % of the field without the FSTs, on plasmas. Thus, fortunately, the non-linearity was small and the time for iteration due to the effect of the FSTs is acceptable for a real-time control. On the other hand, the effect on the magnetic sensors is still large, about 10 %, and should be take into account in the calculation for the precise position control since the distance between the FSTs and the magnetic sensor is very close.

So far, a sequence for the equilibrium calculation in the JT-60U consisted of the FBI code and the SELENE code because of the historical reason (due to a limited computing resources in an old system). FBI is a code to determine the plasma boundary and to calculate other related values using a filament current method. SELENE is a code to calculate the equilibrium by using the parameters from diagnostics and FBI outputs. We revised the system of FBI-SELENE to that of CCS-SELENE, namely we replaced the FBI code to the CCS code to minimize the modification of the entire code investments for the experimental data analysis. And the SELENE code was revised in order to take into account the effect of the FSTs in the way similar to the CCS code as mentioned above. Here, $t - \Delta t$ in eq. 1 is one iteration step before the step in this off-line analysis.

An example of the reconstructed plasma shape is shown in FIG. 4. The FSTs were installed on the upper position in the low field side. Thus, the effect is expected to appear in the upper part of plasma. In the region, the viewing chord of the Charge Exchange Recombination Spectroscopy (CXRS) [16] exists. The last closed flux surface (LCFS) location evaluated from CXRS was consistent with the reconstructed LCFS in an H-mode phase as shown in Fig. 4. The reconstructed plasma shape calculated by the new code was also compared with the diagnostics such as a motional stark effect measurement (MSE), Thomson scattering measurement, divertor probes, and their data also consistent with the reconstructed LCFS, considering their errors.

4. Initial experimental results after ferritic insertion

Though we had experience on JFT-2M, we had some concerns about a discharge with the ferritic steel since the installation on a large tokamak is the first experience. We resumed a plasma operation from the beginning of November 2005 after typical conditioning processes, such as a baking of the vacuum vessel at 300°C, wall conditioning by the combination of the Taylor discharge cleaning (TDC) and the glow discharge cleaning (GDC), etc. as usual. The

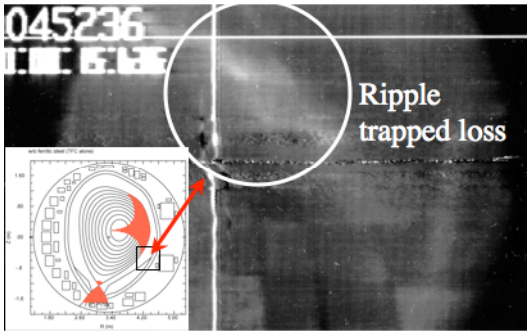

FIG. 5. IRTV camera image viewing the ripple trapped loss region after 1.5s NBI with 22MW. Temperature increment was much small and less than 20 °C.

ohmic plasmas were successfully obtained and were controlled by using the above-mentioned real-time control without a special procedure. In the discharges, no obvious increase in oxygen impurity due to the FSTs was observed, and no obvious effect on Z_{eff} was also observed in the similar plasma shape. This situation was kept during NB heated plasmas.

We have also investigated the improvement of the energetic ion confinement. In the previous work, we confirmed that the OFMC code could well explain the heat load on the first wall by a ripple trapped loss [6,17]. After the FST installation, the heat load measurement was compared with the F3D OFMC simulation. The heat load was measured by an infrared (IR) TV camera. The measured temperature increment for a discharge of E45236 was very small, and less than 20 °C for 1.5 s injection with the power of 22MW as shown in Fig. 5, and this indicates the heat load of less than 0.2 MW/m^2. This amount of the heat load is consistent with the simulated result of less than 0.3 MW/m^2 with FSTs, while the heat flux of above 1MW/m^2 is estimated for without FSTs.

Some of other benefits due to the ferritic insertion were observed from the early time of this campaign. The measurements of the toroidal rotation and the pedestal temperature suggested an increase of toroidal rotation control capability and an improvement of the pedestal pressure [18]. Additionally, the improved confinement of energetic ions have brought a result of β_N~2.3 sustained for 28.6 s [19]. Also, plasmas with high β_N exceeding ideal limit were obtained due to the large co-rotation after installing FSTs [20].

5. Summary

In the further pursuit of steady-state advanced tokamak research on JT-60U, the reduction of the TF ripple was a key issue in large volume plasmas. The reduction of energetic ion loss due to the TF ripple reduction brings: the increase of heating “effective” efficiency, the extended pulse length of RF injection due to the reduced heat flux on antennas and improved coupling between antennas and a plasma with a smaller gap, the availability of wall stabilization without losing heating power, and so on. Based on the useful experience on JFT-2M, the installation of ferritic steel was proposed to improve the energetic ion confinement through reducing a TF ripple. Aiming at cost-effective installation, orbit following calculations of energetic ions were carried out for a design of the installation of ferritic steel on JT-60U by using the F3D OFMC code, which was developed for ferritic insert experiments on JFT-2M and can treat complex magnetic field structure produced by ferritic inserts. In the design work, calculations were carried out for several trial designs, taking into account the limitations from the coexistence with current equipments and the mechanical assessment. As a result, FSTs were installed in place of graphite armors as the first wall by about 10% surface area.

The installed FSTs add the non-linear magnetic field on magnetic sensors for a plasma control and an equilibrium calculation. We revised a real-time control system based on the CCS code. The non-linearity is small in the case of JT-60U because the effect of the magnetic field by FSTs is very small on the plasma, while the effect on the magnetic sensors is still large, about

10%. By using the modified CCS system, we have successfully carried out a real-time plasma control that takes into account the magnetic field by ferritic steel for the first time.

The plasma operation was successfully resumed after usual preparation processes without a special procedure. As a direct benefit of the ferritic insertion, the heat load measurement using IRTV indicated the improved confinement of energetic ions. Additionally, other benefits due to the ferritic insertion were also observed, which will lead to the further extension of the performance on JT-60U.

These results are important for practical application of ferritic steel that is a leading candidate of a structural material on a demo reactor.

Acknowledgment

We would like to thank Mr. H. Hosoyama of the JAEA, and Mr. H. Itakura of the CSK Systems Corporation for their support in the coding of the equilibrium code.

Reference

[1] ITER PHYSICS EXPERT GROUP ON ENERGETIC PARTICLES, HEATING AND CURRENT DRIVE, Nucl. Fusion **39** (1999) 2471.
[2] BASIUK, V., et. al., Nucl Fusion **44** (2004) 181.
[3] TOBITA, K., et. al., Nucl. Fusion **35** (1995) 1585
[4] KAWASHIMA, H., et. al., Nucl. Fusion **41** (2001) 257.
[5] SHINOHARA, K., et.al., Fusion Sci. Tech., **49** 187 (2006)
[6] SHINOHARA, K., et. al., Nucl. Fusion **43** 586 (2003)
[7] TSUZUKI, K., et.al., Fusion Sci. Tech., **49** 197 (2006)
[8] IKEDA, Y., et. al., Nucl. Fusion **36** 759 (1996).
[9] SHINOHARA, K., et. al., Plasma Fusion Res. **1** 007 (2006)
[10] KUDO, Y., et. al., to be published in Journal of Korean Physical Society (2006)
[11] SAKURAI, S., et al., Fusion Eng. and Design **39-40** (1998) 371.
[12] SHIBAMA, Y. K. et. al., submitted to Fusion Eng. and Design.
[13] KURIHARA, K., Fusion. Eng. and Design 51-52 (2000) 1049.
[14] URATA, K., et. al., JAERI-Data/Code 2004-007, 1-45 (2004) (in Japanese).
[15] KAMEARI, A., and POPA, R. C., " "EMSolution": A program for three-dimensional electromagnetic analysis", presented at 2nd Japanese-Bulgarian-Macedonian Joint Seminar on Applied Electromagnetics November 1-3, 1999, Sapporo.
[16] KOIDE, Y., et.al., Rev. Sci. Instrum. **72**, 119 (2001)
[17] TOBITA, K.,et. al., Phys. Rev. Lett. **69** 3060 (1992)
[18] URANO, H., et.al., Fusion Energy 2006 (Proc. 21st Int. Conf. Chengdu, 2006), IAEA-CN-149/EX/5-1, IAEA
[19] OYAMA, N. et.al., Fusion Energy 2006 (Proc. 21st Int. Conf. Chengdu, 2006), IAEA-CN-149/EX/1-3, IAEA
[20] TAKECHI, M. et.al., Fusion Energy 2006 (Proc. 21st Int. Conf. Chengdu, 2006), IAEA-CN-149/EX/7-1Rb, IAEA